The Journal of Pathology: Clinical Research
J Pathol Clin Res March 2025; **11**: e70021
Published online in Wiley Online Library
(wileyonlinelibrary.com). DOI: 10.1002/2056-4538.70021

BRIEF REPORT

Sarcomatoid areas of urothelial carcinoma are enriched for CD163-positive antigen-presenting cells

Burles A Johnson III[1,2], Vamsi Parimi[3], Sonia Kamanda[3], David C Corney[4], Woonyoung Choi[2,5], Jean Hoffman-Censits[1,2,5], Max Kates[1,2,5], David J McConkey[1,2,5], Noah M Hahn[1,2,5] and Andres Matoso[1,2,3,5]*

[1]*Department of Oncology, The Johns Hopkins Medical Institutions, Baltimore, Maryland, USA*
[2]*Department of Urology, Johns Hopkins Greenberg Bladder Cancer Institute, Baltimore, Maryland, USA*
[3]*Department of Pathology, The Johns Hopkins Medical Institutions, Baltimore, Maryland, USA*
[4]*Multiomics, Azenta Life Sciences, South Plainfield, New Jersey, USA*
[5]*Department of Urology, The Johns Hopkins Medical Institutions, Baltimore, Maryland, USA*

**Correspondence to: Andres Matoso, Department of Pathology, Johns Hopkins Hospital, Weinberg Building, Room 2243, 401 N. Broadway, Baltimore, MD 21231, USA. E-mail: amatoso1@jhmi.edu*

Abstract

Sarcomatoid urothelial carcinoma (SUC) is a rare histologic subtype with poor prognosis. While there is known intra-tumoral heterogeneity between individual SUC tumors, the relationship between sarcomatoid and conventional urothelial carcinoma (CUC) within the same patient is poorly understood. The objective of this study was to identify differences between the sarcomatoid and CUC tumor microenvironment components that may drive this aggressive phenotype. Using tissue microarrays from eight patient tumors with mixed CUC and SUC, we examined paired CUC, mixed urothelial carcinoma (UC) regions, and SUC using the Nanostring Digital Spatial Profiling platform. We found SUC and mixed UC had higher levels of stromal cells, predominately macrophages and fibroblasts, when compared with CUC within the same tumor. CD14, CD163, and transforming growth factor-beta levels were significantly higher in SUC than in CUC. Immunohistochemical analysis revealed consistently moderate to strong expression of CD163-positive antigen-presenting cells (APCs) in SUC regions, whereas CD68-positive APC expression was generally absent. Thus, in mixed histology SUC, the SUC component preferentially expressed CD163-positive APCs and fibroblasts compared to the CUC component. As CD163-positive APCs and fibroblasts are known to be tumor-promoting and immune-suppressive, this infiltration may contribute to epithelial to mesenchymal transition and other aggressive properties of SUC.

Keywords: sarcomatoid carcinoma; bladder cancer; macrophage; CD163

Received 25 October 2024; Revised 24 January 2025; Accepted 29 January 2025

Conflicts of interest statement: The authors disclose that they have no significant relationships with or financial interest in any commercial companies pertaining to this article, except for DCC who is an employee and shareholder in Azenta which offers NanoString Digital Spatial Profiling as a service.

Introduction

Sarcomatoid urothelial carcinoma (SUC) is a rare, aggressive subtype of urothelial carcinoma (UC) that is morphologically distinct and comprises 5% or less of UC [1]. Although neoadjuvant chemotherapy in muscle-invasive SUC results in a 38% pathologic complete response, there is overall a high recurrence rate [2]. Moreover, retrospective analyses indicate that SUC has a poor prognosis when compared with conventional urothelial carcinoma (CUC) [3].

The aggressive behavior of SUC has traditionally been thought to be derived from the epithelial to mesenchymal transition (EMT) of tumor cells, which is the transformation of polarized epithelial cells into cells with a mesenchymal phenotype with an increased capacity to migrate, invade, and survive, including vimentin, collagen pathways, and TGF-β among others [4,5]. Over the last few decades, it has become clear that the tumor microenvironment (TME), which includes nonmalignant cells of the stroma and immune cells, is a critical player in cancer progression [6]. With the approval of immune checkpoint inhibitors (ICIs) for bladder cancer therapy, there has been a renewed interest in understanding the characteristics of the tumor immune TME to be able to predict therapy response [7–10].

Here, we used digital spatial profiling to compare the gene expression profile between the carcinomatous and sarcomatoid components within the same tumor, aimed at providing further insight into the changes leading to the more aggressive phenotype, and validated the results using immunohistochemistry (IHC).

Materials and methods

This study was approved by the institutional review board of Johns Hopkins Hospital with waved consent from patients (IRB00369136). The clinicopathologic characteristics of patients are presented in Table 1. Tumors from 8 of these patients were used for digital spatial profiling, and tumors from all 30 patients for IHC.

Specimens and digital spatial profiling

Tissue microarrays were constructed using formalin-fixed paraffin-embedded specimens from eight patients with mixed urothelial carcinoma and sarcomatoid carcinoma (Figure 1A). Paired CUC and sarcomatoid carcinoma were analyzed utilizing Nanostring Digital Spatial Profiling using the cancer transcriptome atlas assay that includes 1,800 mRNA targets. Immunofluorescence analysis using anti-pancytokeratin antibody to identify cancer cells and anti-CD45 to identify lymphoid cells was used to aid cell selection (Figure 1A). Cores with regions of interest (ROIs) were selected in real time based on histology and annotated as epithelioid/urothelial carcinoma ($n = 26$), sarcomatoid ($n = 18$), and mixed ($n = 15$), by expert urologic pathologists (SK and AM) (Figure 1B). Datasets were annotated and categorized as either sarcomatoid, epithelial, or mixed. Data quality control (QC) was performed to identify ROIs with low coverage, low numbers of cells, etc. Of 59 ROIs, 54 passed QC. A linear mixed model with Benjamini-Hochberg correction for multiple hypothesis testing was applied to the ROIs to identify differentially expressed genes (22 ROIs epithelial, 17 ROIs sarcomatoid, and 15 ROIs mixed). Pathway analysis was performed on the differentially expressed genes.

Table 1. Clinicopathologic characteristics of the patients

Total number of patients (*n*)	30
Age (years)	68 (range 42–90)
Male:Female	2.8:1
Race (%)	
White	83
African American	14
Asian	3
Average tumor size (cm)	6
Average tumor size (cm) of sarcomatoid component	4.8
Heterologous elements in sarcomatoid component (%)	12
Other associated histologic subtypes (%)	
Squamous cell carcinoma	20
Glandular/plasmacytoid/signet ring cell	10
Micropapillary	6
Small cell/large cell neuroendocrine	3
Pathologic stage (%)	
pT1	6
pT2	36
pT3	41
pT4	17
Surgical resection (%)	
Total cystectomy	70
Partial cystectomy	7
Pelvic exenteration	3
NAC and AC (%)	87
Overall survival (months)	14 (range 1–198)

AC, adjuvant chemotherapy; NAC, neoadjuvant chemotherapy.

Immunohistochemistry

Immunohistochemical stains were performed at Johns Hopkins Hospital on a Roche Ventana Benchmark Ultra automated stainer (Ventana Medical Systems, Tucson, AZ, USA) for CD68 (clone KP-1, predilute, Ventana), and on the Leica BOND-III (Leica Biosystems, Deer Park, IL, USA) for CD163 (clone 1,006, dilution 1:500, Leica Biosystems). Antigen retrieval was performed using CC1 buffer (cell conditioning 1; citrate buffer pH 6.0, Ventana), and detection was achieved using the UltraMap DAB detection kit (Roche Diagnostics Corporation, Indianapolis, IN, USA). Staining for CD68 and CD163 was used to assess tumor-infiltrating macrophages and as surrogate markers of macrophage subpopulations classically activated (M1, CD68) or alternatively activated (M2, CD163) [11,12]. Tumor-infiltrating macrophages were scored as negative/mild when there were ≤5 positive cells per high-power field (HPF), moderate when there were 5–50 positive cells per HPF, and strong when there were ≥50 positive cells per HPF.

Results

Digital spatial profiling allows for discriminatory assessment of gene expression profiles in areas of tumors with different morphology. Differentially expressed genes were identified between sarcomatoid, mixed, and epithelial ROIs. Pathway enrichment analysis revealed enrichment of extracellular matrix-related pathways within sarcomatoid ROIs. Unbiased hierarchical

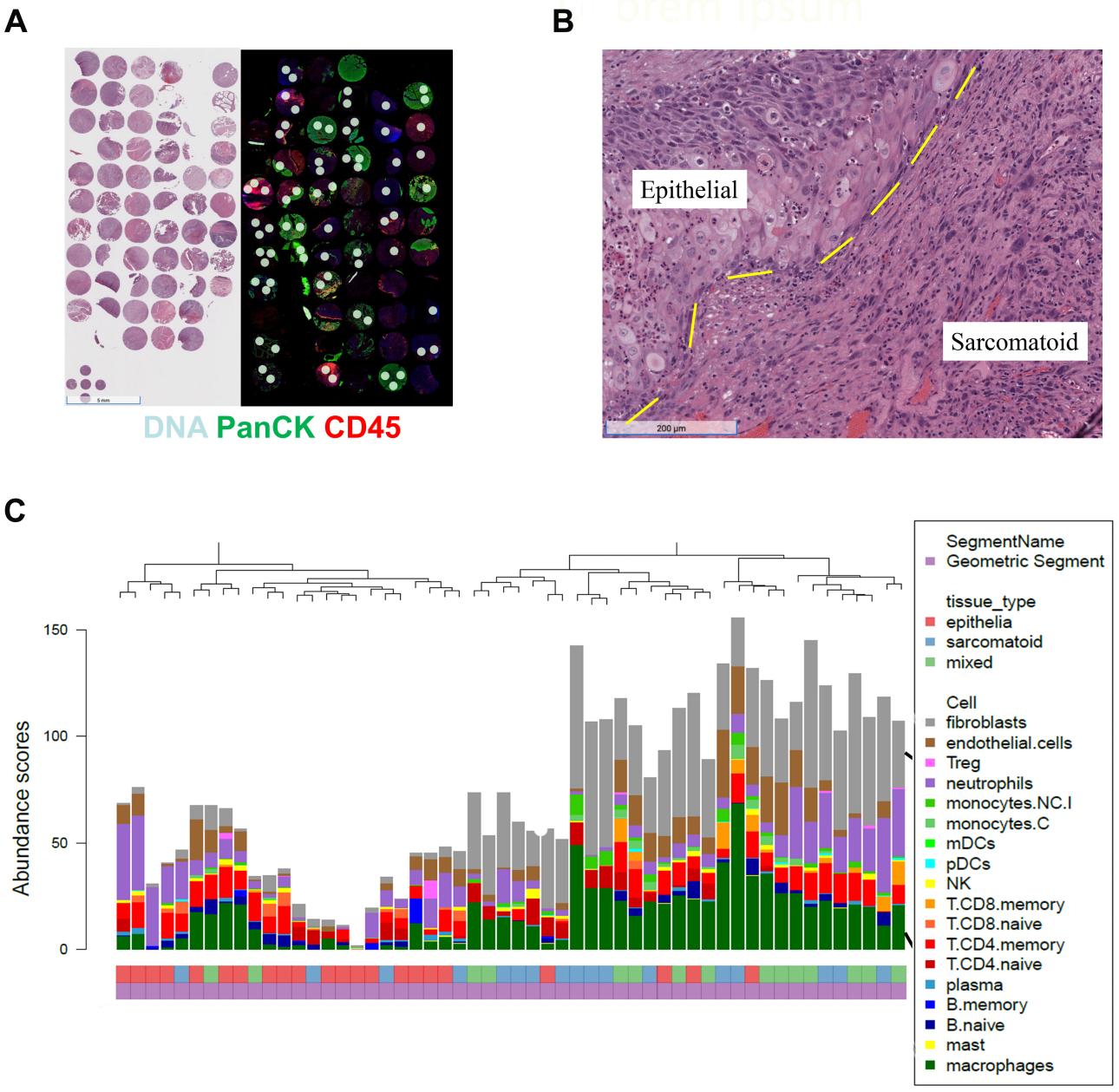

Figure 1. Digital spatial profiling (DSP) analysis. (A) Tissue microarrays (TMA) with urothelial and sarcomatoid areas from the same patients. Hematoxylin and eosin-stained (H&E) TMA (left) used to select epithelioid and sarcomatoid areas for analysis. Immunofluorescence analysis using anti-pancytokeratin antibody (green) to select cancer cells, anti-CD45 (red) to identify lymphoid cells, and anti-DNA antibody (light gray) to highlight cell nuclei. White circles indicate areas selected as regions of interest (ROIs). (B) H&E-stained area showing the transition between epithelioid and sarcomatoid areas in the same tumor selected for DSP. (C) Pathway analysis comparing carcinoma and sarcomatoid areas showed a more pronounced macrophage and fibroblast signature in the sarcomatoid areas, although there are some cases in which the epithelioid areas show prominent macrophage infiltration.

clustering of stromal abundance in SUC, mixed, and CUC revealed that 18 of 24 CUC clustered together, and 26 of 30 SUC or mixed tumors clustered together (Figure 1C). Spatial deconvolution of stromal cell types in the ROIs determined there was a higher total stromal infiltrate in most SUC and mixed UC when compared with the CUC component (Figure 1C). This appeared to be driven by a high abundance of fibroblasts and macrophages, which were present at higher levels in SUC and mixed UC when compared with

CUC (Figure 1C). There were 8 of 32 SUC and mixed UC ROI (compared with 3 of 22 CUC) that had high neutrophil abundance but, overall, there was not a significant difference between expression in SUC/mixed UC and CUC. T cells were present but not significantly different between SUC and CUC, and B cells, NK, and mast cells were minimally present in most samples (Figure 1C).

To further evaluate the role of macrophages in SUC, we compared mRNA expression of selected macrophage genes between SUC and CUC within each tumor. In SUC, there was higher expression of CD14 ($p = 0.0005$), which is a pan-macrophage marker also expressed on some neutrophils and dendritic cells [13]. Also in SUC, there was higher expression of CD163 ($p = 0.001$), which is expressed by immune suppressive antigen-presenting cells (APCs), along with CD68 ($p = 0.0004$) and TNF-α ($p = 0.004$), which are generally associated with immune stimulatory APCs [14]. Finally, in the SUC component, there was significantly higher expression of transforming growth factor beta (TGFβ; $p = 0.049$), which is secreted by immune suppressive macrophages as well as cancer associated fibroblasts [15]. There was no difference in *CD274* (encoding PD-L1) expression between SUC and CUC areas.

To confirm the above findings, we performed IHC for CD163 and CD68 in tumors from 30 patients

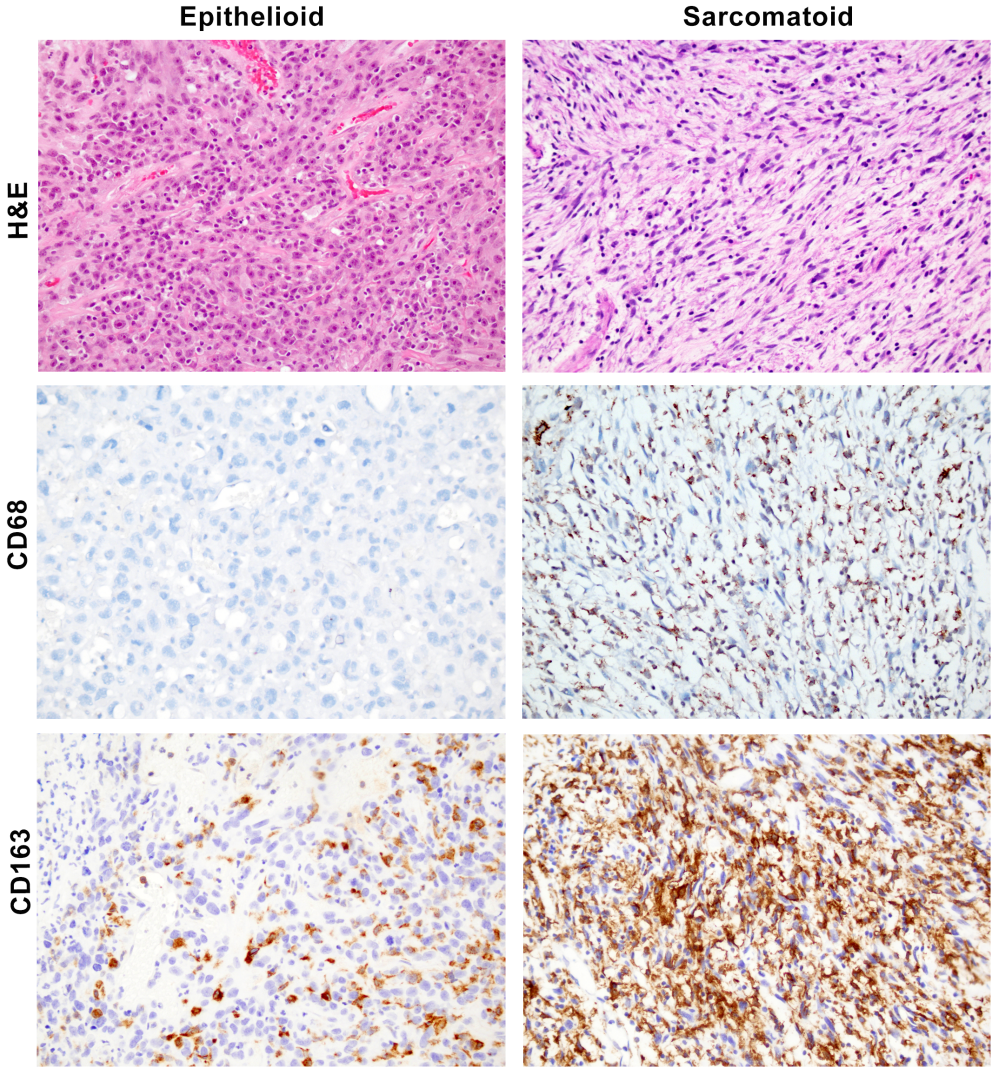

Figure 2. Immunohistochemical staining for CD68 and CD163. The top row shows H&E-stained sections showing epithelioid (left) and sarcomatoid (right) areas of the same tumor. The middle row shows immunostaining for CD68, and the bottom row shows the same areas as the top and middle rows but stained for CD163, demonstrating stronger and more diffuse staining compared with CD68.

including the 8 tumors used for the TMA, with a focus on the SUC component. Infiltration of CD163-positive APCs was significantly higher than CD68-positive APCs ($p < 0.001$). Staining for CD163 was strong in 13 of 30 cases (44%), and moderate in the remaining 17 of 30 (56%). Conversely, staining for CD68 was negative in 27 of 30 cases (87%) and mild to moderate in 3 of 30 cases (13%). Thus, CD163-positive APCs predominate in SUC (Figure 2).

Discussion

This study demonstrates that (1) stromal infiltration is overall greater in the SUC component when compared with conventional UC in mixed histology SUC, (2) this stromal infiltration is dominated by macrophages and fibroblasts, and (3) CD163-positive APCs predominate over CD68-positive APCs in the SUC component.

The value of this analysis is that it used spatial profiling to compare the SUC component with the conventional UC component within the same tumor. Previous comparisons of SUC with conventional UC within the same tumor indicated upregulation of EMT, which is associated with tumor aggressiveness [16]. In addition, comprehensive analysis of 28 SUC and 84 CUC also identified an EMT signature as a primary characteristic of SUC [17]. This study extends these findings by implicating fibroblasts and CD163-positive APCs, which both drive EMT, as the predominant immune infiltrate in SUC. Additionally, TGFβ is commonly produced by both of these cell types [15], and this cytokine is known to drive EMT and tumorigenicity in UC [18]. Thus, EMT could be driven by these two cell types. Previous studies have identified an immune-suppressive macrophage gene signature in SUC using bulk RNA molecular analyses but did not confirm this with Immunohistochemical analyses of macrophage markers [17]. Our study found a pronounced macrophage infiltration (and comparatively few B cells) in most SUC components, which contrasts SUC with a recent report of spatial transcriptomic profiling in conventional muscle-invasive UC, where B cells predominated (along with macrophages in a subset of tumors) [19].

Our IHC studies have demonstrated higher tumor infiltration of CD163-positive macrophages than CD68-positive macrophages in the sarcomatoid component. CD163 has been identified as a marker of macrophages with immunosuppressive and tumor progression features [12]. Notably, one of the cytokines associated with the activation of this tumor progression pathway is TGFβ, which was also identified as significantly more highly expressed in the sarcomatoid component of tumors. TGFβ is known for playing a significant role in EMT, epithelial plasticity, and invasive properties of cancer cells. A previous study has emphasized the potential role of EMT in the aggressive biology of SUC, demonstrating that tumor cells gain expression of certain EMT-associated markers including foreheadbox protein C2 (FOXC2), SNAIL, and SEB1, while they lose expression of epithelial derived markers including N- and E-cadherins [20].

This study has several limitations, including a small sample size with low statistical power, reliance on samples from a single institution, and the absence of separate training and test cohorts, among others. However, its strengths lie in the fact that the findings are based on comparisons within the same tumor, which helps to identify differences more likely associated with sarcomatoid transformation. In conclusion, our study demonstrates that brisk infiltration of CD163-positive macrophages in the sarcomatoid areas could be a critical determinant of its clinical aggressiveness.

Acknowledgements

This work was supported by a National Institutes of Health Institutional Research Training Grant (T32 CA193145, to VP and SK), a Department of Defense Career Development Award (CA220769, to BAJ), and Maryland Cigarette Restitution Fund Award (to BAJ).

Author contributions statement

BJ and AM designed the study and wrote the manuscript. VP, SK and DCC performed the experiments and analyzed the data. WC, JH-C, MK, DJM and NMH performed critical review of the data and the manuscript.

Data availability statement

Raw data are provided in supplementary material, Table S1.

References

1. Netto GJ, Amin MB, Berney DM, *et al*. The 2022 World Health Organization classification of tumors of the urinary system and

male genital organs-part B: prostate and urinary tract tumors. *Eur Urol* 2022; **82**: 469–482.
2. Johnson Iii BA, Teply BA, Kagemann C, *et al*. Neoadjuvant cisplatin, gemcitabine, and docetaxel in Sarcomatoid bladder cancer: clinical activity and whole transcriptome analysis. *Bladder Cancer* 2024; **10**: 133–143.
3. Wright JL, Black PC, Brown GA, *et al*. Differences in survival among patients with sarcomatoid carcinoma, carcinosarcoma and urothelial carcinoma of the bladder. *J Urol* 2007; **178**: 2302–2306.
4. Yun SJ, Kim WJ. Role of the epithelial-mesenchymal transition in bladder cancer: from prognosis to therapeutic target. *Korean J Urol* 2013; **54**: 645–650.
5. Kalluri R, Weinberg RA. The basics of epithelial-mesenchymal transition. *J Clin Invest* 2009; **119**: 1420–1428.
6. Quail DF, Joyce JA. Microenvironmental regulation of tumor progression and metastasis. *Nat Med* 2013; **19**: 1423–1437.
7. Chen Z, Chen D, Song Z, *et al*. Mapping the tumor microenvironment in bladder cancer and exploring the prognostic genes by single-cell RNA sequencing. *Front Oncol* 2022; **12**: 1105026.
8. Li Y, Liu Y, Kang Z, *et al*. Tumor microenvironment heterogeneity in bladder cancer identifies biologically distinct subtypes predicting prognosis and anti-PD-L1 responses. *Sci Rep* 2023; **13**: 19563.
9. Martins-Lima C, Chianese U, Benedetti R, *et al*. Tumor microenvironment and epithelial-mesenchymal transition in bladder cancer: cytokines in the game? *Front Mol Biosci* 2022; **9**: 1070383.
10. Chen Z, Qin C, Wang G, *et al*. A tumor microenvironment preoperative nomogram for prediction of lymph node metastasis in bladder cancer. *Front Oncol* 2022; **12**: 1099965.
11. Biswas SK, Sica A, Lewis CE. Plasticity of macrophage function during tumor progression: regulation by distinct molecular mechanisms. *J Immunol* 2008; **180**: 2011–2017.
12. Heusinkveld M, van der Burg SH. Identification and manipulation of tumor associated macrophages in human cancers. *J Transl Med* 2011; **9**: 216.
13. Sharygin D, Koniaris LG, Wells C, *et al*. Role of CD14 in human disease. *Immunology* 2023; **169**: 260–270.
14. Chen S, Saeed A, Liu Q, *et al*. Macrophages in immunoregulation and therapeutics. *Signal Transduct Target Ther* 2023; **8**: 207.
15. Deng Z, Fan T, Xiao C, *et al*. TGF-beta signaling in health, disease, and therapeutics. *Signal Transduct Target Ther* 2024; **9**: 61.
16. Genitsch V, Kollar A, Vandekerkhove G, *et al*. Morphologic and genomic characterization of urothelial to sarcomatoid transition in muscle-invasive bladder cancer. *Urol Oncol* 2019; **37**: 826–836.
17. Guo CC, Majewski T, Zhang L, *et al*. Dysregulation of EMT drives the progression to clinically aggressive sarcomatoid bladder cancer. *Cell Rep* 2019; **27**: 1781–1793.e4.
18. Sim WJ, Iyengar PV, Lama D, *et al*. c-Met activation leads to the establishment of a TGFbeta-receptor regulatory network in bladder cancer progression. *Nat Commun* 2019; **10**: 4349.
19. Eyers M, Irlam J, Marshall G, *et al*. Digital spatial profiling of the microenvironment of muscle invasive bladder cancer. *Commun Biol* 2024; **7**: 737.
20. Sanfrancesco J, McKenney JK, Leivo MZ, *et al*. Sarcomatoid urothelial carcinoma of the bladder: analysis of 28 cases with emphasis on clinicopathologic features and markers of epithelial-to-mesenchymal transition. *Arch Pathol Lab Med* 2016; **140**: 543–551.

SUPPLEMENTARY MATERIAL ONLINE

Table S1. Raw data